LETTER Communicated by Valerie Ventura

Information-Geometric Measures as Robust Estimators of Connection Strengths and External Inputs

Masami Tatsuno
tatsunom@nsma.arizona.edu
Arizona Research Laboratories, Division of Neural Systems, Memory and Aging, University of Arizona, Tucson, AZ 85724, U.S.A., and Laboratory for Mathematical Neuroscience, RIKEN Brain Science Institute, Wako, Saitama 351-0198, Japan

Jean-Marc Fellous
fellous@email.arizona.edu
Arizona Research Laboratories, Division of Neural Systems, Memory and Aging; Department of Psychology; and Evelyn F. McKnight Brain Institute, University of Arizona, Tucson, AZ 85724, U.S.A.

Shun-ichi Amari
amari@brain.riken.jp
Laboratory for Mathematical Neuroscience, RIKEN Brain Science Institute, Wako, Saitama 351-0198, Japan

Information geometry has been suggested to provide a powerful tool for analyzing multineuronal spike trains. Among several advantages of this approach, a significant property is the close link between information-geometric measures and neural network architectures. Previous modeling studies established that the first- and second-order information-geometric measures corresponded to the number of external inputs and the connection strengths of the network, respectively. This relationship was, however, limited to a symmetrically connected network, and the number of neurons used in the parameter estimation of the log-linear model needed to be known. Recently, simulation studies of biophysical model neurons have suggested that information geometry can estimate the relative change of connection strengths and external inputs even with asymmetric connections. Inspired by these studies, we analytically investigated the link between the information-geometric measures and the neural network structure with asymmetrically connected networks of N neurons. We focused on the information-geometric measures of orders one and two, which can be derived from the two-neuron log-linear model, because unlike higher-order measures, they can be easily estimated experimentally. Considering the equilibrium state of a network of binary model neurons that obey stochastic dynamics, we analytically showed that the corrected

first- and second-order information-geometric measures provided robust and consistent approximation of the external inputs and connection strengths, respectively. These results suggest that information-geometric measures provide useful insights into the neural network architecture and that they will contribute to the study of system-level neuroscience.

1 Introduction

To understand how populations of neurons interact in the brain, it is important to record from as many neurons as possible simultaneously. Due to recent technological developments, multielectrode recordings have become a standard tool in electrophysiology, enabling the recording of spiking activity from tens to hundreds of neurons simultaneously (Wilson & McNaughton, 1993; Hoffman & McNaughton, 2002; Nicolelis & Ribeiro, 2002; Buzsaki, 2004). To understand how simultaneously recorded spikes are related to the dynamics of cell assemblies, a number of data analysis techniques have been proposed (Gerstein & Perkel, 1969; Abeles & Gerstein, 1988; Aertsen, Gerstein, Habib, & Palm, 1989; Riehle, Grün, Diesmann, & Aertsen, 1997; Zhang, Ginzburg, McNaughton, & Sejnowski, 1998; Nadasdy, Hirase, Czurko, Csicsvari, & Buzsaki, 1999; Louie & Wilson, 2001; Grün, Diesmann, & Aertsen, 2002; Brown, Kass, & Mitra, 2004; Fellous, Tiesinga, Thomas, & Sejnowski, 2004; Czanner, Grün, & Iyengar, 2005; Kass, Ventura, & Brown, 2005; Tatsuno, Lipa, & McNaughton, 2006; Shimazaki & Shinomoto, 2007; Houghton & Sen, 2008). Among those, information-geometric analyses of multineuronal spike data have been actively studied (Nakahara & Amari, 2002; Amari, Nakahara, Wu, & Sakai, 2003; Tatsuno & Okada, 2004; Eleuteri, Tagliaferri, & Milano, 2005; Ikeda, 2005; Miura, Okada, & Amari, 2006; Nakahara, Amari, & Richmond, 2006) since the original proposal by Amari (2001).

Isolated pairs and triplets of model neurons were used (Ginzburg & Sompolinsky, 1994) to investigate the possible relationship between the information-geometric measures and some of the features of the underlying neural architectures such as the connection strengths and the number of external inputs (Tatsuno & Okada, 2004). This study showed that for symmetrically connected networks, the first- and second-order information-geometric measures directly represented the external inputs, and the connection strengths, respectively, provided that the number of neurons used in the parameter estimation of the log-linear model was known. For asymmetric networks, however, the information-geometric measures were shown to be dependent on both the connection strengths and the external inputs. In other words, the information-geometric measures could not disentangle the connection strengths and the external inputs correctly for asymmetrically connected networks.

In an effort to develop an analytical framework for the characterization of multineuronal spike patterns, we have also proposed a novel method by integrating spike train clustering (Fellous et al., 2004) and information geometry (Lipa, Tatsuno, Amari, McNaughton, & Fellous, 2006; Lipa, Tatsuno, McNaughton, & Fellous, 2007). In these studies, ensemble spike trains were generated with asymmetric recurrent networks of biophysical model neurons connected by AMPA and $GABA_A$ synapses. We found not only that the clustering method successfully identified subgroups of neurons that were characterized by partial temporal correlations but also that the information-geometric method correctly estimated the relative change of connection strengths and external inputs even with asymmetric connections (Lipa et al., 2006, 2007). This finding leads to the theoretical investigations of information geometry that are presented here.

In this study, we show that the difficulty for the general asymmetric case can be corrected by analytically approximating the bias term that arises from interactions with many other neurons. In addition, we show that the information-geometric measures based on the two-neuron log-linear model can be used in a network of N neurons, avoiding the complexity of using the multineuronal log-linear model.

2 Information-Geometric Measures

We provide a brief introduction to the information-geometric method; detailed descriptions can be found elsewhere (Amari, 2001; Nakahara & Amari, 2002).

Information geometry is a subfield of probability theory that has emerged from investigations of the geometrical structures of the parameter space of probability distributions (Amari, 1985; Amari & Nagaoka, 2000). Utilizing a hierarchical structure in an exponential family or mixture family of distributions, Amari (2001) proposed an orthogonal decomposition of interactions among random variables. When a spike train is represented as binary random variables, the joint probability distribution of N-neuronal firings $p_{x_1 x_2,\ldots,x_N}$ can be represented by the log-linear model: $\log p_{x_1 x_2,\ldots,x_N}$ is expanded as

$$\log p_{x_1 x_2 \ldots x_N} = \sum_i \theta_i^{(N)} x_i + \sum_{i<j} \theta_{ij}^{(N)} x_i x_j + \sum_{i<j<k} \theta_{ijk}^{(N)} x_i x_j x_k + \cdots + \theta_{1\ldots N}^{(N)} x_1, \ldots, x_N - \psi^{(N)}, \tag{2.1}$$

where x_i is a binary variable representing neural firing of the ith neuron and $\theta_{1,2,\ldots,k}^{(N)}$ represent the kth order neural interactions among N neurons.

The first few terms of $\theta^{(N)}$ coefficients and $\psi^{(N)}$ are expressed as

$$\begin{aligned}
\theta_i^{(N)} &= \log \frac{p_{x_1=0,\ldots,x_i=1,\ldots,x_N=0}}{p_{x_1=0,\ldots,x_N=0}} \\
\theta_{ij}^{(N)} &= \log \frac{p_{x_1=0,\ldots,x_i=1,\ldots,x_j=1,\ldots,x_N=0}\, p_{x_1=0,\ldots,x_N=0}}{p_{x_1=0,\ldots,x_i=1,\ldots,x_j=0,\ldots,x_N=0}\, p_{x_1=0,\ldots,x_i=0,\ldots,x_j=1,\ldots,x_N=0}} \\
\theta_{ijk}^{(N)} &= \log \frac{p_{x_1=0,\ldots,x_i=1,\ldots,x_j=1,\ldots,x_k=1,\ldots,x_N=0}\, p_{x_1=0,\ldots,x_i=1,\ldots,x_j=0,\ldots,x_k=0,\ldots,x_N=0}}{p_{x_1=0,\ldots,x_i=1,\ldots,x_j=1,\ldots,x_k=0,\ldots,x_N=0}\, p_{x_1=0,\ldots,x_i=0,\ldots,x_j=1,\ldots,x_k=1,\ldots,x_N=0}} \\
&\quad \times \frac{p_{x_1=0,\ldots,x_i=0,\ldots,x_j=1,\ldots,x_k=0,\ldots,x_N=0}\, p_{x_1=0,\ldots,x_i=0,\ldots,x_j=0,\ldots,x_k=1,\ldots,x_N=0}}{p_{x_1=0,\ldots,x_i=1,\ldots,x_j=0,\ldots,x_k=1,\ldots,x_N=0}\, p_{x_1=0,\ldots,x_N=0}} \\
&\quad \ldots \\
\psi^{(N)} &= -\log p_{x_1=0,\ldots,x_N=0},
\end{aligned} \tag{2.2}$$

where $0 \le i < j < k \le N$. In practice, estimates of θs are obtained as functions of maximum likelihood estimates of $p_{x_1 x_2,\ldots,x_N}$, given by

$$p_{x_1 x_2,\ldots,x_N} = \frac{n_{x_1 x_2,\ldots,x_N}}{\sum_{x_1,\ldots,x_N} n_{x_1 x_2,\ldots,x_N}}, \tag{2.3}$$

where $n_{x_1 x_2,\ldots,x_N}$ is the number of trials in which the event $(X_1 = x_1, X_2 = x_2, \ldots, X_N = x_N)$ occurs.

In real experiments, N, the number of interacting neurons that belong to the network in which the recorded cells are embedded is expected to be large but is unknown. Therefore, we cannot assume the specific number N for the log-linear model. Furthermore, because the number of $\theta^{(N)}$ parameters in the log-linear model increases as $2^N - 1$, it is difficult to obtain a robust estimation of all the parameters for large N. Therefore, in this study, we focus on the information-geometric measures $\theta_1^{(2)}$, $\theta_2^{(2)}$, and $\theta_{12}^{(2)}$ of the two-neuron log-linear model,

$$\log p_{x_1 x_2} = \theta_1^{(2)} x_1 + \theta_2^{(2)} x_2 + \theta_{12}^{(2)} x_1 x_2 - \psi^{(2)}, \tag{2.4}$$

which includes interactions with other $N - 2$ neurons implicitly. The parameters of the two-neuron model are given by

$$\theta_1^{(2)} = \log \frac{p_{10}}{p_{00}}, \quad \theta_2^{(2)} = \log \frac{p_{01}}{p_{00}}, \quad \theta_{12}^{(2)} = \log \frac{p_{11} p_{00}}{p_{10} p_{01}}, \quad \psi^{(2)} = -\log p_{00}. \tag{2.5}$$

Note that $p_{x_1 x_2}$ obtained from the N-neuron model is

$$p_{x_1 x_2} = \sum_{x_3,\ldots,x_N} p_{x_1 x_2,\ldots,x_N}, \tag{2.6}$$

and the parameters $\theta_1^{(2)}$, $\theta_2^{(2)}$, and $\theta_{12}^{(2)}$ in equation 2.5 are different from $\theta_1^{(N)}$, $\theta_2^{(N)}$, and $\theta_{12}^{(N)}$ in equation 2.2. The two-neuron model gives the marginal distribution of the N-neuron model. When this simple model is considered, the number of parameters that need to be estimated reduces to three. Since the above two neurons are members of an N-neuron network, $\theta_1^{(2)}$, $\theta_2^{(2)}$, and $\theta_{12}^{(2)}$ will be affected by the other $N-2$ neurons. By calculating these interaction terms from the other $N-2$ neurons, the method becomes applicable in realistic experimental conditions. In the following, we investigate in detail how $\theta_i^{(2)}$ and $\theta_{ij}^{(2)}$ are related to the external inputs and the connection strengths in the general N-neuron network, with both symmetric and asymmetric connections.

3 Model Network

Following the previous study (Tatsuno & Okada, 2004), we adopt a network of stochastic model neurons studied by Ginzburg and Sompolinsky (1994). The simplicity of the model allows us to study the relationship between the information-geometric measures and the network architectures analytically. In this section, we briefly introduce the model. A more detailed exposition can be found elsewhere (Ginzburg & Sompolinsky, 1994).

The state of each neuron at time t takes one of two values, 0 or 1, corresponding to a quiescent and active state, respectively. The total input to the ith neuron at time t is written as

$$u_i(t) = \sum_{j=1}^{N} J_{ij} S_j(t) + h_i, \tag{3.1}$$

where J_{ij} denotes the connection strength from the jth presynaptic neuron to the ith postsynaptic one, and h_i represents the external input to the ith neuron. We assume that there is no self-coupling (i.e., $J_{ii} = 0$) following the previous studies (Ginzburg & Sompolinsky, 1994; Tatsuno & Okada, 2004), but the effect of self-coupling is negligible in the analysis with a large N limit. The neuron dynamics is determined by the transition rate w between the binary states as

$$\begin{aligned} w(S_i = 0 \to S_i = 1) &= \frac{1}{\tau_0} g(u_i), \\ w(S_i = 1 \to S_i = 0) &= \frac{1}{\tau_0}(1 - g(u_i)), \\ w(S_i = 0 \to S_i = 0) &= 1 - w(0 \to 1), \\ w(S_i = 1 \to S_i = 1) &= 1 - w(1 \to 0), \end{aligned} \tag{3.2}$$

where τ_0 is a microscopic characteristic time constant and $g(u_i)$ is a monotonically increasing smooth activation function such as

$$g(u_i) = \frac{1 + \tanh(\beta(u_i - m))}{2}, \tag{3.3}$$

where $\beta > 0$ and m are constants determining the slope and offset threshold of the sigmoid. The probability of finding the system in a state $P(S_1, \ldots, S_N, t)$ at time t is then provided by the following master equation:

$$\frac{d}{dt}P(S_1, \ldots, S_N, t) = -\sum_{i=1}^{N} w(S_i \to (1 - S_i))P(S_1, \ldots, S_N, t) + \sum_{i=1}^{N} w((1 - S_i) \to S_i)P(S_1 \ldots, 1 - S_i, \ldots, S_N, t). \tag{3.4}$$

4 First- and Second-Order Information-Geometric Measures and Network Parameters

4.1 Network of Two Neurons. Before we discuss a general N neuron case, it is instructive to summarize the results from a simple example of two-neuron networks. Here, we briefly show the results (the detailed derivation can be found in Tatsuno & Okada, 2004).

For an asymmetrically connected two-neuron network, the mean firing rate of each neuron in the equilibrium state is obtained as

$$\langle S_1 \rangle = \frac{g(h_1) + \Delta g_1 g(h_2)}{1 - \Delta g_1 \Delta g_2}, \tag{4.1}$$

$$\langle S_2 \rangle = \frac{g(h_2) + \Delta g_2 g(h_1)}{1 - \Delta g_1 \Delta g_2}, \tag{4.2}$$

where $\Delta g_1 = g(J_{12} + h_1) - g(h_1)$ and $\Delta g_2 = g(J_{21} + h_2) - g(h_2)$, respectively. Because the right-hand sides of equations 4.1 and 4.2 involve J_{12}, J_{21}, h_1, and h_2 only, the mean firing rate is expressed by the network parameters. Using $\langle S_1 \rangle$ and $\langle S_2 \rangle$, the mean coincident firing rate is also given as

$$\langle S_1 S_2 \rangle = \frac{1}{2}\{\langle S_1 \rangle g(J_{21} + h_2) + \langle S_2 \rangle g(J_{12} + h_1)\}. \tag{4.3}$$

The firing rates ($\langle S_1 \rangle$, $\langle S_2 \rangle$) and the covariance are related in a nontrivial manner to the external input (h_1, h_2) and the connection strength (J_{12}, J_{21}).

For the two-neuron information-geometric measure, the joint probability distribution is related to the above quantities by

$$\begin{aligned} p_{00} &= 1 - \langle S_1 \rangle - \langle S_2 \rangle + \langle S_1 S_2 \rangle, \\ p_{01} &= \langle S_2 \rangle - \langle S_1 S_2 \rangle, \\ p_{10} &= \langle S_1 \rangle - \langle S_1 S_2 \rangle, \\ p_{11} &= \langle S_1 S_2 \rangle. \end{aligned} \tag{4.4}$$

Substituting these into equation 2.5 and using equation 3.3 gives analytical expressions for the two-neuron information-geometric measures in terms of the network parameters,

$$\begin{aligned}
\theta_1^{(2,A2)} &= 2\beta(h_1 - m) \\
&\quad + \log\left(\frac{2\exp[2\beta(h_1+h_2+J_{12})] + 2\exp[4\beta m] + 2\exp[2\beta(h_1+J_{12}+m)]}{\exp[2\beta(h_1+h_2+J_{12})] + \exp[2\beta(h_1+h_2+J_{21})] + 2\exp[4\beta m]}\right. \\
&\quad \left.\times\frac{+\exp[2\beta(h_2+J_{12}+m)] + \exp[2\beta(h_2+J_{21}+m)]}{+2\exp[2\beta(h_1+J_{12}+m)] + 2\exp[2\beta(h_2+J_{21}+m)]}\right), \\
\theta_2^{(2,A2)} &= 2\beta(h_2 - m) \\
&\quad + \log\left(\frac{2\exp[2\beta(h_1+h_2+J_{21})] + 2\exp[4\beta m] + 2\exp[2\beta(h_2+J_{21}+m)]}{\exp[2\beta(h_1+h_2+J_{12})] + \exp[2\beta(h_1+h_2+J_{21})] + 2\exp[4\beta m]}\right. \\
&\quad \left.\times\frac{+\exp[2\beta(h_1+J_{12}+m)] + \exp[2\beta(h_1+J_{21}+m)]}{+2\exp[2\beta(h_1+J_{12}+m)] + 2\exp[2\beta(h_2+J_{21}+m)]}\right), \\
\theta_{12}^{(2,A2)} &= \beta(J_{12}+J_{21}) \\
&\quad + \log\left(\frac{(\exp[2\beta(h_1+h_2+J_{12})] + \exp[2\beta(h_1+h_2+J_{21})] + 2\exp[2\beta m]}{(2\exp[2\beta(h_1+h_2+J_{12})] + 2\exp[4\beta m] + 2\exp[2\beta(h_1+J_{12}+m)]}\right. \\
&\quad \times\frac{+2\exp[2\beta(h_1+J_{12}+m)] + 2\exp[2\beta(h_2+J_{21}+m)])(2\exp[\beta(2h_1+2h_2+J_{12}+J_{21})]}{+\exp[2\beta(h_2+J_{12}+m)] + \exp[2\beta(h_2+J_{21}+m)])(2\exp[2\beta(h_1+h_2+J_{21})]} \\
&\quad \times\frac{+2\exp[\beta(2h_1+J_{12}+J_{21}+2m)] + 2\exp[2h_2+J_{12}+J_{21}+2m]}{+2\exp[4\beta m] + \exp[2\beta(h_1+J_{12}+m)] + \exp[2\beta(h_1+J_{21}+m)]} \\
&\quad \left.\times\frac{+\exp[\beta(J_{12}-J_{21}+4m)] + \exp[\beta(J_{21}-J_{12}+4m)])}{+2\exp[2\beta(h_2+J_{21}+m)])}\right). \qquad (4.5)
\end{aligned}$$

Here the superscript (2, A2) means that the information-geometric measures are calculated with the two-neuron log-linear model in an asymmetrically connected two-neuron network. The first-order information-geometric measures ($\theta_1^{(2,A2)}$, $\theta_2^{(2,A2)}$) are expressed by the term corresponding to the external input and an additional logarithmic bias term. Similarly, the second-order information-geometric measure $\theta_{12}^{(2,A2)}$ has the term corresponding to the sum of the connection strength and an additional logarithmic bias term.

If we assume the symmetric connection ($J_{12} = J_{21}$), the above expression is significantly simplified as

$$\theta_1^{(2,S2)} = 2\beta(h_1 - m), \quad \theta_2^{(2,S2)} = 2\beta(h_2 - m), \quad \theta_{12}^{(2,S2)} = 2\beta J_{12}. \qquad (4.6)$$

These equations show that the first- and second-order information-geometric measures correspond to the external inputs and the connection strengths, respectively, as previously shown (Tatsuno & Okada, 2004).

4.2 Network of *N* Neurons. In the previous section, we already see that complexity differs significantly for asymmetric and symmetric connections

(see equations 4.5 and 4.6) for even a simple two-neuron network. Because the analytical expressions for the asymmetrically connected N neurons will be extremely complicated, we first investigate the analytical results for the symmetrically connected N neuron case. We then extend our investigations to the asymmetric case.

Tatsuno and Okada (2004) showed that if the number of neurons of the log-linear model (two in our case) and that of the network N differs, the simple relationships in equation 4.6 no longer hold even for symmetric networks. For example, the two-neuron log-linear model in a symmetrically connected three-neuron network generates $\theta^{(2,S3)}$, which has additional bias terms as

$$\begin{aligned}
\theta_1^{(2,S3)} &= 2\beta\,(h_1 - m) + \log\frac{1+\exp\left[2\beta\left((h_3 - m) + J_{13}\right)\right]}{1+\exp\left[2\beta\,(h_3 - m)\right]},\\
\theta_2^{(2,S3)} &= 2\beta\,(h_2 - m) + \log\frac{1+\exp\left[2\beta\left((h_3 - m) + J_{23}\right)\right]}{1+\exp\left[2\beta\,(h_3 - m)\right]},\\
\theta_{12}^{(2,S3)} &= 2\beta J_{12} + \log\frac{(1+\exp[2\beta(h_3 - m)])(1+\exp[2\beta((h_3 - m) + J_{13} + J_{23})])}{(1+\exp[2\beta((h_3 - m) + J_{13})])(1+\exp[2\beta((h_3 - m) + J_{23})])}.
\end{aligned} \tag{4.7}$$

Note the difference between equations 4.5 and 4.7; the logarithmic term in equation 4.5 arises from asymmetric connections in two-neuron networks, while the logarithmic term in equation 4.7 stems from the third neuron of symmetrically connected three-neuron networks. Note also that the information-geometric measures calculated by the three-neuron log-linear model, $\theta^{(3,S3)}$, are expressed as

$$\theta_1^{(3,S3)} = 2\beta\,(h_1 - m)\,, \quad \theta_2^{(3,S3)} = 2\beta\,(h_2 - m)\,, \quad \theta_{12}^{(3,S3)} = 2\beta J_{12}, \tag{4.8}$$

involving the external input and the connection strength separately.

The above three-neuron network example suggests that the two-neuron information-geometric measure $\theta^{(2,S3)}$ does not represent the network architectures exactly. However, if the second logarithmic bias term in equation 4.7 is approximated, the corrected $\theta^{(2,S3)}$ would provide a consistent approximation of the external inputs and the connection strengths. We therefore investigate the two-neuron log-linear model in a symmetrically connected N-neuron network. By simple calculation, extending equation 4.7 to the N neuron case yields a general relationship as

$$\begin{aligned}
\theta_1^{(2,SN)} = 2\beta\,(h_1 - m) + \log\Bigg(&\frac{1+\sum_{j=3}^{N}\exp\left[2\beta\left((h_j - m) + J_{1j}\right)\right]}{1+\sum_{j=3}^{N}\exp\left[2\beta\,(h_j - m)\right]}\\
&\times\frac{+\sum_{i=3}^{N-1}\sum_{j>i}^{N}\exp\left[2\beta((h_i - m) + (h_j - m) + J_{1i} + J_{1j} + J_{ij})\right]}{+\sum_{i=3}^{N-1}\sum_{j>i}^{N}\exp\left[2\beta((h_i - m) + (h_j - m) + J_{ij})\right]}
\end{aligned}$$

$$\times \frac{+\cdots+\exp\left[2\beta\left(\sum_{i=3}^{N}(h_i-m)+\sum_{i=1,\neq 2}^{N-1}\sum_{j>i,\neq 2}^{N}J_{ij}\right)\right]}{+\cdots+\exp\left[2\beta\left(\sum_{i=3}^{N}(h_i-m)+\sum_{i=3}^{N-1}\sum_{j>i}^{N}J_{ij}\right)\right]}\Bigg),$$

$$\theta_2^{(2,SN)} = 2\beta(h_2-m)+\log\Bigg(\frac{1+\sum_{j=3}^{N}\exp\left[2\beta\left((h_j-m)+J_{2j}\right)\right]}{1+\sum_{j=3}^{N}\exp\left[2\beta(h_j-m)\right]}$$

$$\times \frac{+\sum_{i=3}^{N-1}\sum_{j>i}^{N}\exp\left[2\beta((h_i-m)+(h_j-m)+J_{1i}+J_{1j}+J_{ij})\right]}{+\sum_{i=3}^{N-1}\sum_{j>i}^{N}\exp\left[2\beta((h_i-m)+(h_j-m)+J_{ij})\right]}$$

$$\times \frac{+\cdots+\exp\left[2\beta\left(\sum_{i=3}^{N}(h_i-m)+\sum_{i=2}^{N-1}\sum_{j>i}^{N}J_{ij}\right)\right]}{+\cdots+\exp\left[2\beta\left(\sum_{i=3}^{N}(h_i-m)+\sum_{i=3}^{N-1}\sum_{j>i}^{N}J_{ij}\right)\right]}\Bigg),$$

$$\theta_{12}^{(2,SN)} = 2\beta J_{12}+\log\Bigg(\frac{\left(1+\sum_{j=3}^{N}\exp\left[2\beta\left((h_j-m)+J_{1j}+J_{2j}\right)\right]\right.}{\left(1+\sum_{j=3}^{N}\exp\left[2\beta\left((h_j-m)+J_{ij}\right)\right]\right.}$$

$$\times \frac{+\sum_{i=3}^{N-1}\sum_{j>i}^{N}\exp\left[2\beta\left((h_i-m)+(h_j-m)+J_{1i}+J_{1j}+J_{2i}+J_{2j}+J_{ij}\right)\right]}{+\sum_{i=3}^{N-1}\sum_{j>i}^{N}\exp\left[2\beta\left((h_i-m)+(h_j-m)+J_{1i}+J_{1j}+J_{ij}\right)\right]}$$

$$\times \frac{+\cdots+\exp\left[2\beta\left(\sum_{i=3}^{N}(h_i-m)+\sum_{i=1}^{N-1}\sum_{j>i,\neq 2}^{N}J_{ij}\right)\right]\Big)\left(1+\sum_{j=3}^{N}\exp\left[2\beta(h_j-m)\right]\right.}{+\cdots+\exp\left[2\beta\left(\sum_{i=3}^{N}(h_i-m)+\sum_{i=1,\neq 2}^{N-1}\sum_{j>i,\neq 2}^{N}J_{ij}\right)\right]\Big)\left(1+\sum_{j=3}^{N}\exp\left[2\beta\left((h_j-m)+J_{ij}\right)\right]\right.}$$

$$\times \frac{+\sum_{i=3}^{N-1}\sum_{j>i}^{N}\exp\left[2\beta\left((h_i-m)+(h_j-m)+J_{ij}\right)\right]}{+\sum_{i=3}^{N-1}\sum_{j>i}^{N}\exp\left[2\beta\left((h_i-m)+(h_j-m)+J_{1i}+J_{1j}+J_{ij}\right)\right]}$$

$$\times \frac{+\cdots+\exp\left[2\beta\left(\sum_{i=3}^{N}(h_i-m)+\sum_{i=3}^{N-1}\sum_{j>i}^{N}J_{ij}\right)\right]\Big)}{+\cdots+\exp\left[2\beta\left(\sum_{i=3}^{N}(h_i-m)+\sum_{i=2}^{N-1}\sum_{j>i}^{N}J_{ij}\right)\right]\Big)}\Bigg). \tag{4.9}$$

Equation 4.9 gives the relationship between $\theta^{(2,SN)}$ and the parameters of the network of the model neurons h_i, J_{ij}, β, and m. In the following sections, we first approximate the logarithmic term for a uniformly connected network and then extend the analysis to nonuniformly connected asymmetric connections.

5 Uniformly Connected N Neuron Networks

As a special case of symmetric connections, we start with a network with uniform connections and uniform external inputs. By letting $h_i = h$ and $J_{ij} = J$, equation 4.9 is reduced to

$$\theta_1^{(2,UN)} = \theta_2^{(2,UN)} = 2\beta(h-m)+\log\frac{\sum_{i=0}^{N-2}{}_{N-2}C_i\exp\left[2\beta\left(i\,(h-m)+\frac{i(i+1)}{2}J\right)\right]}{\sum_{i=0}^{N-2}{}_{N-2}C_i\exp\left[2\beta\left(i\,(h-m)+\frac{i(i-1)}{2}J\right)\right]}$$

$$= 2\beta\,(h-m)+\log\frac{A_+}{A_-},$$

$$\begin{aligned}\theta_{12}^{(2,UN)} &= 2\beta J + \log\left(\frac{\sum_{i=0}^{N-2} {}_{N-2}C_i \exp\left[2\beta\left(i\,(h-m)+\frac{i(i+3)}{2}J\right)\right]}{\sum_{i=0}^{N-2} {}_{N-2}C_i \exp\left[2\beta\left(i\,(h-m)+\frac{i(i+1)}{2}J\right)\right]}\right.\\ &\quad\left.\times\frac{\sum_{i=0}^{N-2} {}_{N-2}C_i \exp\left[2\beta\left(i\,(h-m)+\frac{i(i-1)}{2}J\right)\right]}{\sum_{i=0}^{N-2} {}_{N-2}C_i \exp\left[2\beta\left(i\,(h-m)+\frac{i(i+1)}{2}J\right)\right]}\right)\\ &= 2\beta J + \log\frac{A_{3+}A_{-}}{A_{+}^2},\end{aligned} \tag{5.1}$$

where ${}_{N-2}C_i$ is a binomial coefficient and

$$\begin{aligned}A_{\pm} &= \sum_{i=0}^{N-2} {}_{N-2}C_i \exp\left[2\beta\left(i\,(h-m)+\frac{i\,(i\pm 1)}{2}J\right)\right],\\ A_{3+} &= \sum_{i=0}^{N-2} {}_{N-2}C_i \exp\left[2\beta\left(i\,(h-m)+\frac{i\,(i+3)}{2}J\right)\right].\end{aligned} \tag{5.2}$$

In this study, we investigate the fully connected networks where each neuron is connected to all other neurons. Therefore, we consider the case where each connection is weak, typically on the order of $1/N$. Otherwise the total synaptic inputs will drive the neuron into saturation. By Stirling's approximation,

$$N! = \sqrt{2\pi N}N^N e^{-N}\left\{1+O\left(\frac{1}{N}\right)\right\}, \tag{5.3}$$

and by rewriting$N' = N-2$, $J = c/N$, and $i = (N-2)r = N'r$, we obtain

$$\begin{aligned}{}_{N-2}C_i &= {}_{N'}C_{N'r}\\ &= \frac{1}{\sqrt{2\pi N'r(1-r)}}\exp\left[N'\left\{-r\log r-(1-r)\log(1-r)\right\}\right]\\ &\quad\times\left\{1+O\left(\frac{1}{N'}\right)\right\}\\ &= \frac{1}{\sqrt{2\pi N'r(1-r)}}\exp\left[N'H(r)\right]\left\{1+O\left(\frac{1}{N'}\right)\right\},\end{aligned} \tag{5.4}$$

where $H(r) = -r\log r - (1-r)\log(1-r)$. Note that this approximation is accurate when N' is large. We then obtain

$$\begin{aligned}
A &\equiv \sum_{i=0}^{N-2} {}_{N-2}C_i \exp\left[2\beta\left(i\,(h-m) + \frac{i^2}{2}J\right)\right] \\
&= \sum_{\substack{r=0 \\ \frac{1}{N'}step}}^{1} \frac{1}{\sqrt{2\pi N' r(1-r)}} \exp\left[N'H(r) + 2\beta N'(h-m)r + \beta(N'r)^2 J\right] \\
&\quad \times \left\{1 + O\left(\frac{1}{N'}\right)\right\} \\
&= \sum_{r} \exp\left[N'\left\{H(r) + 2\beta(h-m)r + \beta c r^2 - \frac{1}{2N'}\log N'\right.\right. \\
&\quad \left.\left. -\frac{1}{2N'}\log(2\pi r(1-r))\right\}\right]\left\{1 + O\left(\frac{1}{N'}\right)\right\} \\
&= \sum_{r} \exp\left[N' f(r)\right]\left\{1 + O\left(\frac{1}{N'}\right)\right\}, \qquad (5.5)
\end{aligned}$$

where $f(r) = H(r) + 2\beta(h-m)r + \beta c r^2 - \log N'/(2N') - \log(2\pi r(1-r))/(2N')$.

To investigate further, by taking a large N' limit, we approximate equation 5.5 using a continuous variable r. With Taylor's expansion, A is written as

$$\begin{aligned}
A &\approx \int_0^1 \exp[N' f(r)]\left\{1 + O\left(\frac{1}{N'}\right)\right\} dr \\
&= \int_0^1 \exp\left[N'\left\{f(r_0) + \frac{1}{2}f''(r_0)(r-r_0)^2 + \frac{1}{6}f^{(3)}(r_0)(r-r_0)^3\right.\right. \\
&\quad \left.\left. + \frac{1}{24}f^{(4)}(r_0)(r-r_0)^4 + O((r-r_0)^5)\right\}\right] \\
&\quad \times \left\{1 + O\left(\frac{1}{N'}\right)\right\} dr \\
&\approx \exp[N' f(r_0)] \int_{-\infty}^{\infty} \exp\left[\frac{N'}{2}\left\{f''(r_0)(r-r_0)^2 + \frac{1}{3}f^{(3)}(r_0)(r-r_0)^3\right.\right. \\
&\quad \left.\left. + \frac{1}{12}f^{(4)}(r_0)(r-r_0)^4 + O((r-r_0)^5)\right\}\right] \\
&\quad \times \left\{1 + O\left(\frac{1}{N'}\right)\right\} dr \\
&= \exp\left[N' f(r_0)\right] G(r_0), \qquad (5.6)
\end{aligned}$$

where r_0 is given by $r_0 = \arg\max_r f(r)$, yielding

$$\log \frac{1-r_0}{r_0} + 2\beta(h-m) + 2\beta c r_0 = 0, \tag{5.7}$$

and $G(r_0)$ is given by

$$\begin{aligned} G(r_0) = \int_{-\infty}^{\infty} \exp\Bigg[\frac{N'}{2}\Bigg\{ & f''(r_0)(r-r_0)^2 + \frac{1}{3}f^{(3)}(r_0)(r-r_0)^3 \\ & + \frac{1}{12}f^{(4)}(r_0)(r-r_0)^4 + O((r-r_0)^5)\Bigg\}\Bigg] \\ & \times \left\{1 + O\left(\frac{1}{N'}\right)\right\} dr. \end{aligned} \tag{5.8}$$

When a new variable u is defined as

$$u = \sqrt{N'}r, \tag{5.9}$$

$G(r_0)$ is written as

$$\begin{aligned} G(u_0) = \frac{1}{\sqrt{N'}} \int_{-\infty}^{\infty} \exp\Bigg[\frac{1}{2}\Bigg\{ & f''(u_0)(u-u_0)^2 + \frac{1}{3}f^{(3)}(u_0)\frac{(u-u_0)^3}{\sqrt{N'}} \\ & + \frac{1}{12}f^{(4)}(u_0)\frac{(u-u_0)^4}{N'} + O\left(\frac{1}{N'\sqrt{N'}}\right)\Bigg\}\Bigg] \\ & \times \left\{1 + O\left(\frac{1}{N'}\right)\right\} du. \end{aligned} \tag{5.10}$$

Since the integral of the $(u-u_0)^3$ term is 0 and that of the $(u-u_0)^4$ term is in $O(1/N')$, $G(u_0)$ is given as

$$\begin{aligned} G(u_0) &= \frac{1}{\sqrt{N'}} \int_{-\infty}^{\infty} \exp\left[\frac{1}{2}\left\{f''(u_0)(u-u_0)^2 + O\left(\frac{1}{N'}\right)\right\}\right] \\ &\quad \times \left\{1 + O\left(\frac{1}{N'}\right)\right\} du \\ &= \int_{-\infty}^{\infty} \exp\left[\frac{N'}{2}f''(r_0)(r-r_0)^2\right]\left\{1 + O\left(\frac{1}{N'}\right)\right\} dr. \end{aligned} \tag{5.11}$$

With the saddle point approximation, we have

$$G(r_0) \approx \sqrt{\frac{2\pi}{N'|f''(r_0)|}} \left\{1 + O\left(\frac{1}{N'}\right)\right\}. \tag{5.12}$$

Thus, A is given as

$$A = \exp\left[N' f(r_0)\right] \sqrt{\frac{2\pi}{N'|f''(r_0)|}} \left\{1 + O\left(\frac{1}{N'}\right)\right\}. \tag{5.13}$$

$A_{\pm}$ and A_{3+} are similarly calculated as

$$\begin{aligned}
A_{\pm} &= \sum_r \exp\left[N' f(r) \pm \beta c r\right] \left\{1 + O\left(\frac{1}{N'}\right)\right\} \\
&\approx \int \exp\left[N' f(r) \pm \beta c r\right] \left\{1 + O\left(\frac{1}{N'}\right)\right\} dr \\
&\approx A \exp\left[\pm \beta c r_0\right] \left\{1 + O\left(\frac{1}{N'}\right)\right\}, \\
A_{3+} &= \sum_r \exp\left[N' f(r) + 3\beta c r\right] \left\{1 + O\left(\frac{1}{N'}\right)\right\} \\
&\approx \int \exp\left[N' f(r) + 3\beta c r\right] \left\{1 + O\left(\frac{1}{N'}\right)\right\} dr \\
&\approx A \exp\left[3\beta c r_0\right] \left\{1 + O\left(\frac{1}{N'}\right)\right\}.
\end{aligned} \tag{5.14}$$

Therefore, we obtain

$$\begin{aligned}
\log \frac{A_+}{A_-} &= \log \frac{A \exp\left[\beta c r_0\right] \left\{1 + O\left(\frac{1}{N'}\right)\right\}}{A \exp\left[-\beta c r_0\right] \left\{1 + O\left(\frac{1}{N'}\right)\right\}} \\
&= \log \left(\exp\left[2\beta c r_0\right] \left\{1 + O\left(\frac{1}{N'}\right)\right\} \right) \\
&= 2\beta c r_0 + O\left(\frac{1}{N'}\right),
\end{aligned} \tag{5.15}$$

and similarly,

$$\begin{aligned}
&\log \frac{A_{3+} A_-}{A_+^2} \\
&= \log \frac{\left(A \exp\left[3\beta c r_0\right] \left\{1 + O\left(\frac{1}{N'}\right)\right\}\right) \left(A \exp\left[-\beta c r_0\right] \left\{1 + O\left(\frac{1}{N'}\right)\right\}\right)}{\left(A \exp\left[\beta c r_0\right] \left\{1 + O\left(\frac{1}{N'}\right)\right\}\right)^2}
\end{aligned}$$

$$= \log\left(\exp[0]\left\{1 + O\left(\frac{1}{N'}\right)\right\}\right)$$
$$= 0 + O\left(\frac{1}{N'}\right). \tag{5.16}$$

From equations 5.15 and 5.16 and letting $N' = N$ in a large N limit, we obtain

$$\theta_1^{(2,UN)} = \theta_2^{(2,UN)} = 2\beta(h-m) + 2\beta c r_0 + O\left(\frac{1}{N}\right),$$
$$\theta_{12}^{(2,UN)} = 2\beta J + O\left(\frac{1}{N}\right). \tag{5.17}$$

Equation 5.17 shows that in a large N limit, the second logarithmic bias term of the first-order information-geometric measures ($\theta_1^{(2,UN)}$ and $\theta_2^{(2,UN)}$) can be approximated by $2\beta c r_0$ and that the second logarithmic bias term of the second-order information-geometric measure $\theta_{12}^{(2,UN)}$ reduces to 0. $\theta_{12}^{(2,UN)}$ therefore provides a consistent approximation of the connection strengths. By defining the corrected first-order information-geometric measures, $\tilde{\theta}_1^{(2,UN)}$ and $\tilde{\theta}_2^{(2,UN)}$, as

$$\tilde{\theta}_1^{(2,UN)} = \theta_1^{(2,UN)} - 2\beta c r_0,$$
$$\tilde{\theta}_2^{(2,UN)} = \theta_2^{(2,UN)} - 2\beta c r_0, \tag{5.18}$$

we obtain

$$\tilde{\theta}_1^{(2,UN)} = \tilde{\theta}_2^{(2,UN)} = 2\beta(h-m) + O\left(\frac{1}{N}\right), \tag{5.19}$$

which provide a consistent approximation of the external inputs.

To further investigate the bias term $2\beta c r_0$, we calculated r_0 in equation 5.7 by finding an intersecting point between $y = -\log((1-r_0)/r_0)$ and $y = 2\beta(h-m) + 2\beta c r_0$. Because the second equation represents a linear line with a slope of $2\beta c$ with positive β, the number of intersecting points depends on the connection strength parameter$c$. For negative c, there is only one intersecting point. For positive c, in the weak connection range of $c < 2/\beta$, only one intersecting point exists as well. For the strong connection range of $c > 2/\beta$, there are two cases in which only one intersecting point or three intersection points exist, depending on the strength of the external input h.

To calculate the concrete value of r_0, we assume that the network parameters are known. Here, we used biologically plausible parameters following

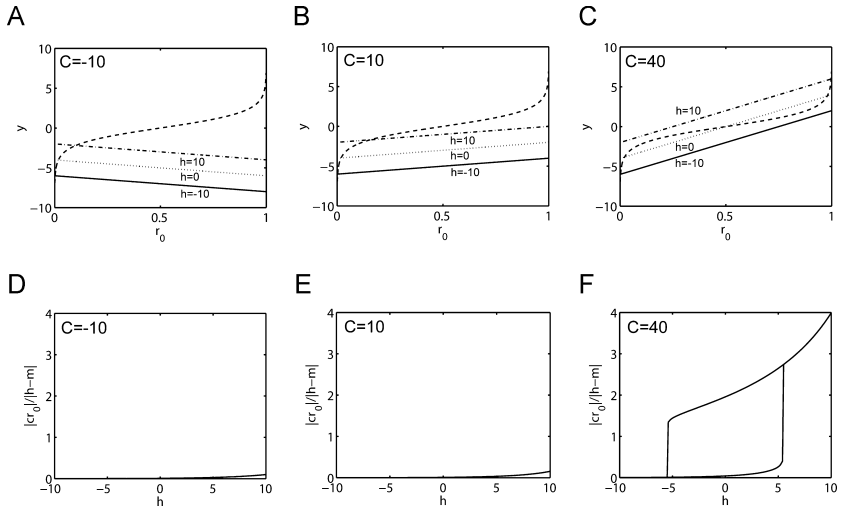

Figure 1: Estimation of r_0 and the relative error of the first-order information-geometric measure ($\theta_1^{(2,UN)}$ and $\theta_2^{(2,UN)}$) for uniformly connected networks. (A) $y = -\log((1-r_0)/r_0)$ (dashed line) and $y = 2\beta(h-m) + 2\beta c r_0$ for $h = -10$ (solid line), $h = 0$ (dotted line), and $h = 10$ (dash-dot line) were plotted for negative connection networks ($c = -10$). An intersection point provides a solution for r_0. (B) Estimation of r_0 for weakly positive connection networks ($c = 10$). (C) Estimation of r_0 for strongly positive connection networks ($c = 40$). Note that there is a transition between one-solution mode and three-solution mode depending on the value of h. (D) Estimation of the relative error $|cr_0|/|h-m|$ for negative connection networks ($c = -10$). (E) Estimation of the relative error for a weakly positive connection network ($c = 10$). (F) Estimation of the relative error for a strongly positive connection network ($c = 40$). Because of bistability of the equilibrium state, the hysteresis is observed.

the discussion in Ginzburg and Sompolinsky (1994): $\beta = 0.1$ and $m = 20$ for the sigmoid function, c in $[-10, 40]$ for the connection strengths, and h in $[-10, 10]$ for the external inputs. Note however, that the following discussion is also valid for other values of β and m.

Figures 1A to 1C show the intersecting points between $y = -\log((1-r_0)/r_0)$ and $y = 2\beta(h-m) + 2\beta c r_0$ for the three typical conditions: the negative connection ($c = -10$), the weakly positive connection ($c = 10$, satisfying $c < 2/\beta$), and the strongly positive connection ($c = 40$, satisfying $c > 2/\beta$), respectively. The dashed line represents $y = -\log((1-r_0)/r_0)$, and the solid, dotted, and dash-dot lines represent $y = 2\beta(h-m) + 2\beta c r_0$ corresponding to the different external input levels of $h = -10$, $h = 0$, and $h = 10$, respectively. For the negative ($c = -10$) and weakly positive connections ($c = 10$), Figures 1A and 1B show that

there is only one solution for r_0, and it monotonically increases with the external input parameter h. For the strongly positive connection ($c = 40$), Figure 1C shows a transition between the one-solution and the three-solution mode, depending on the value of h. Letting the two solutions of $f'(r)$ be r_1 and r_2 ($r_1 < r_2$), a simple calculation yields that when $h < (1/2\beta)\log(r_2/(1-r_2)) - cr_2 + m$ or $h > (1/2\beta)\log(r_1/(1-r_1)) - cr_1 + m$, there is one solution. Otherwise there are three-solutions. Furthermore, because both the smallest and the largest solutions are stable in the three-solution mode, it exhibits hysteresis that depends on the history of the solution. Note also that two stable solutions correspond to the two maxima of $f(r)$, where their values become equal at $h = 0$. Since the saddle point approximation becomes poor when multiple local maxima exist, it would not give a good approximation in the vicinity of $h = 0$. However, except this narrow region where two maxima of $f(r)$ have similar values, the saddle point approximation would give a practically good approximation by choosing the higher maximum of $f(r)$ as the solution for r_0.

Figures 1D to 1F show a relative error measured by the ratio between the effect of interest and the bias term of the right-hand side of the first-order information-geometric measures ($\theta_1^{(2,UN)}$ and $\theta_2^{(2,UN)}$) in equation 5.17,

$$\frac{|2\beta c r_0|}{|2\beta(h-m)|} = \frac{|cr_0|}{|h-m|}. \tag{5.20}$$

For the negative and weakly positive connections, the error increases with h, reaching up to 10% for the negative connection (see Figure 1D) and 16% for the weakly positive connection (see Figure 1E). For the strongly positive connection, the hysteresis emerged because of the bistability of the solutions (see Figure 1F). If the smaller solution is selected, the relative error reaches up to 40%. If the larger solution is chosen, the second bias term is as large as the quantity of interest. However, when the bias term $2\beta c r_0$ is taken into account, the corrected information-geometric measures ($\tilde{\theta}_1^{(2,UN)}$ and $\tilde{\theta}_2^{(2,UN)}$) provide consistent approximations of the external inputs.

To investigate the relationship between r_0 and the equilibrium state and to verify if the network parameters investigated above cover most of the firing rate in the equilibrium state, we calculated the equilibrium state $\bar{S}_i$ from

$$\bar{S}_i = g\left(\sum_{j=1}^{N} J_{ij}\bar{S}_j + h_i\right). \tag{5.21}$$

By letting $J_{ij} = c/N$ and $h_i = h$, we write the equilibrium state as $\bar{S}_i = \bar{S}$, and equation 5.21 reduces to

$$\bar{S} = g(c\bar{S} + h). \tag{5.22}$$

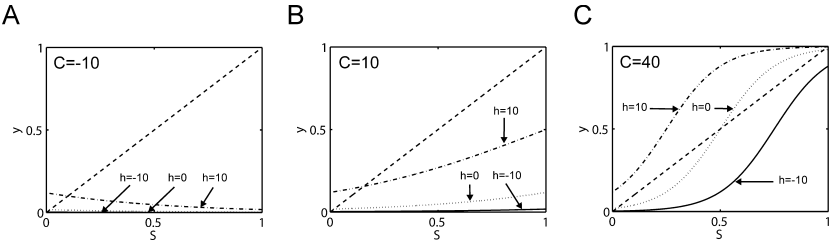

Figure 2: Stability of the equilibrium state of uniformly connected networks. (A) $y = \bar{S}$ (dashed line) and $y = g(c\bar{S} + h)$ for $h = -10$ (solid line), $h = 0$ (dotted line) and $h = 10$ (dash-dot line) were plot for negative connection networks ($c = -10$). An intersecting point provides the solution for $\bar{S}$. When the condition $|g'(c\bar{S} + h)| < 1$ holds, the intersecting point is stable. (B) The equilibrium solution $\bar{S}$ for a weakly positive connection network ($c = 10$). (C) The equilibrium solution $\bar{S}$ for a strongly positive connection network ($c = 40$). Note that there is transition between one-stable-equilibrium state and three-equilibrium states where the smallest and largest ones are stable. Note also that $\bar{S}$ obtained by the investigated network parameters covers practically all firing rate from nearly 0 through almost 1.

Figures 2A to 2C show the intersecting point between $y = \bar{S}$ and $y = g(c\bar{S} + h)$ for the negative connection ($c = -10$), the weakly positive connection ($c = 10$), and the strongly positive connection ($c = 40$), respectively. The intersecting point is stable when the condition $|g'(c\bar{S} + h)| < 1$ holds. As we saw in Figures 1A through 1C, one stable equilibrium state exists for the negative and weakly positive connections (see Figures 2A and 2B), but there is a transition between the one-stable-solution mode and the three-solutions mode for the strongly positive connection (see Figure 2C). It is also clearly seen that the equilibrium state $\bar{S}$ covers practically the entire firing rate range from 0 to 1.

We also derived the relationship between r_0 and $\bar{S}$. From equation 5.7, we obtain

$$\frac{r_0}{1 - r_0} = \exp\left[2\beta\left(cr_0 + h - m\right)\right]. \tag{5.23}$$

Rewriting this equation yields

$$r_0 = \frac{\exp\left[2\beta\left(cr_0 + h - m\right)\right]}{1 + \exp\left[2\beta\left(cr_0 + h - m\right)\right]}. \tag{5.24}$$

As for $\bar{S}$, equation 5.22 yields,

$$\bar{S} = \frac{\exp\left[2\beta\left(c\bar{S} + h - m\right)\right]}{1 + \exp\left[2\beta\left(c\bar{S} + h - m\right)\right]}. \tag{5.25}$$

Thus, this analysis yields the relationship

$$\bar{S} = r_0, \tag{5.26}$$

suggesting that r_0 can be replaced by the equilibrium state $\bar{S}$. This relationship will be useful because $\bar{S}$ can be estimated from observed spike train data.

In summary, the corrected first-order information-geometric measures ($\tilde{\theta}_1^{(2,UN)}$ and $\tilde{\theta}_2^{(2,UN)}$) and the second-order information-geometric measure $\theta_{12}^{(2,UN)}$ provide consistent approximation of the external inputs and the connection strengths, respectively.

6 Nonuniformly and Asymmetrically Connected *N* Neuron Networks

We next consider a nonuniformly connected case, where connections are asymmetric in general. We first write h_i and J_{ij} as the mean and the deviation,

$$\begin{aligned} h_i &= \bar{h} + \varepsilon_i \\ J_{ij} &= \bar{J} + \frac{\varepsilon'_{ij}}{N} = \frac{\bar{c} + \varepsilon'_{ij}}{N}, \end{aligned} \tag{6.1}$$

where $\bar{h}$ and $\bar{J} = \bar{c}/N$ represent their average value, respectively. A, $A_{\pm}$, and A_{3+} are then written as

$$\begin{aligned} A &= \sum_{i=0}^{N-2} {}_{N-2}C_i \exp\left[2\beta \sum_{j=1}^{i} (h_j - m) + \beta \sum_{j=1}^{i^2} J_{ij}\right] \\ A_{\pm} &= \sum_{i=0}^{N-2} {}_{N-2}C_i \exp\left[2\beta \sum_{j=1}^{i} (h_j - m) + \beta \sum_{j=1}^{i^2} J_{ij} \pm \beta \sum_{j=1}^{i} J_{ij}\right] \\ A_{3+} &= \sum_{i=0}^{N-2} {}_{N-2}C_i \exp\left[2\beta \sum_{j=1}^{i} (h_j - m) + \beta \sum_{j=1}^{i^2} J_{ij} + 3\beta \sum_{j=1}^{i} J_{ij}\right]. \end{aligned} \tag{6.2}$$

Here we can rewrite J_{ij} as J_k, k representing index pairs (i,j), without losing generality. A is then calculated as

$$\begin{aligned} A &= \sum_{i=0}^{N-2} {}_{N-2}C_i \exp\left[2\beta \sum_{j=1}^{i} \left((\bar{h} + \varepsilon_j) - m\right) + \beta \sum_{k=1}^{i^2} \left(\frac{\bar{c} + \varepsilon'_k}{N}\right)\right] \\ &= \sum_{r} {}_{N'}C_{N'r} \exp\left[2\beta(\bar{h} - m)N'r + \beta\bar{c}N'r^2 + 2\beta \sum_{j=1}^{N'r} \varepsilon_j + \frac{\beta}{N} \sum_{k=1}^{(N'r)^2} \varepsilon'_k\right] \end{aligned}$$

$$
\begin{aligned}
&= \sum_r \frac{1}{\sqrt{2\pi N' r(1-r)}} \exp\left[N' H(r)\right] \left\{1 + O\left(\frac{1}{N'}\right)\right\} \\
&\quad \times \exp\left[2\beta(\bar{h} - m)N' r + \beta \bar{c} N' r^2 + 2\beta \sum_{j=1}^{N' r} \varepsilon_j + \frac{\beta}{N} \sum_{k=1}^{(N' r)^2} \varepsilon'_k\right] \\
&\approx \sum_r \frac{1}{\sqrt{2\pi N' r(1-r)}} \exp\left[N' \left\{H(r) + 2\beta(\bar{h} - m)r + \beta \bar{c} r^2\right.\right. \\
&\quad \left.\left. + 2\beta\left(\frac{1}{N' r} \sum_{j=1}^{N' r} \varepsilon_j\right) r + \beta\left(\frac{1}{(N' r)^2} \sum_{k=1}^{(N' r)^2} \varepsilon'_k\right) r^2\right\}\right] \\
&\quad \times \left\{1 + O\left(\frac{1}{N'}\right)\right\} \\
&= \sum_r \exp\left[N' \left\{H(r) + 2\beta(\bar{h} - m)r + \beta \bar{c} r^2\right.\right. \\
&\quad \left.\left. - \frac{1}{2N'} \log N' - \frac{1}{2N'} \log\left(2\pi r(1-r)\right) + h_\varepsilon(r) r + J_{\varepsilon'}(r) r^2\right\}\right] \\
&\quad \times \left\{1 + O\left(\frac{1}{N'}\right)\right\} \\
&= \sum_r \exp\left[N' \bar{f}(r)\right] \left\{1 + O\left(\frac{1}{N'}\right)\right\}, \qquad (6.3)
\end{aligned}
$$

where

$$
\begin{aligned}
h_\varepsilon(r) &= \left(\frac{1}{N' r} \sum_{j=1}^{N' r} \varepsilon_j\right), \\
J_{\varepsilon'}(r) &= \left(\frac{1}{(N' r)^2} \sum_{k=1}^{(N' r)^2} \varepsilon'_k\right), \qquad (6.4)
\end{aligned}
$$

and

$$
\begin{aligned}
\bar{f}(r) &= H(r) + 2\beta(\bar{h} - m)r + \beta \bar{c} r^2 - \frac{1}{2N'} \log N' \\
&\quad - \frac{1}{2N'} \log\left(2\pi r(1-r)\right) + h_\varepsilon(r) r + J_{\varepsilon'}(r) r^2. \qquad (6.5)
\end{aligned}
$$

When $h_\varepsilon(r)$ and $h_\varepsilon(r)$ are small, they can be replaced by $h_\varepsilon(r_0)$ and $h_\varepsilon(r_0)$, respectively. Thus, we obtain

$$\bar{f}(r) = H(r) + 2\beta(\bar{h} - m)r + \beta\bar{c}r^2 - \frac{1}{2N'}\log N' - \frac{1}{2N'}\log(2\pi r(1-r)) + h_\varepsilon(r_0)r + J_{\varepsilon'}(r_0)r^2. \tag{6.6}$$

When the saddle point approximation is used,

$$A \approx \int \exp[N'\bar{f}(r)]\left\{1 + O\left(\frac{1}{N'}\right)\right\} dr \approx \exp[N'\bar{f}(\bar{r}_0)]\sqrt{\frac{2\pi}{N'|f''(\bar{r}_0)|}}\left\{1 + O\left(\frac{1}{N'}\right)\right\} \tag{6.7}$$

holds where $\bar{r}_0$ is obtained by $\bar{r}_0 = \arg\max_r \bar{f}(r)$. It yields

$$\log\frac{1-\bar{r}_0}{\bar{r}_0} + 2\beta\left(\bar{h} - m\right) + 2\beta\bar{c}\bar{r}_0 + h_\varepsilon(r_0) + 2J_{\varepsilon'}(r_0)\bar{r}_0 = 0. \tag{6.8}$$

$A_\pm$ and A_{3+} are now calculated as

$$\begin{aligned} A_\pm &= \sum_r {}_{N'}C_{N'r} \exp\left[2\beta\left(\bar{h} - m\right)N'r + \beta\bar{c}N'r^2 + 2\beta\sum_{j=1}^{N'r}\varepsilon_j \right. \\ &\quad \left. + \frac{\beta}{N'}\sum_{k=1}^{(N'r)^2}\varepsilon'_k \pm \left\{\beta\bar{c}r + \frac{\beta}{N'}\sum_{k=1}^{N'r}\varepsilon'_k\right\}\right] \\ &= \sum_r \frac{1}{\sqrt{2\pi N'r(1-r)}} \exp\left[N'\left\{H(r) + 2\beta(\bar{h} - m)r + \beta\bar{c}r^2 \right.\right. \\ &\quad \left.\left. + 2\beta h_\varepsilon(r)r + \beta J_{\varepsilon'}(r)r^2\right\} \pm \left\{\beta\bar{c}r + \beta J^{(1)}_{\varepsilon'}(r)r\right\}\right] \\ &\quad \times \left\{1 + O\left(\frac{1}{N'}\right)\right\} \\ &= \sum_r \exp\left[N'\bar{f}(r) \pm \left\{\beta\bar{c}r + \beta J^{(1)}_{\varepsilon'}(r)r\right\}\right]\left\{1 + O\left(\frac{1}{N'}\right)\right\}, \end{aligned}$$

$$
\begin{aligned}
A_{3+} &= \sum_r {}_{N'}C_{N'r} \exp\left[2\beta\left(\bar{h}-m\right)N'r + \beta\bar{c}N'r^2 + 2\beta\sum_{j=1}^{N'r}\varepsilon_j \right. \\
&\quad \left. + \frac{\beta}{N'}\sum_{k=1}^{(N'r)^2}\varepsilon'_k + 3\left\{\beta\bar{c}r + \frac{\beta}{N'}\sum_{k=1}^{N'r}\varepsilon'_k\right\}\right] \\
&= \sum_r \frac{1}{\sqrt{2\pi N'r(1-r)}} \exp\left[N'\left\{H(r) + 2\beta(\bar{h}-m)r + \beta\bar{c}r^2\right.\right. \\
&\quad \left.\left. + 2\beta h_\varepsilon(r)r + \beta J_{\varepsilon'}(r)r^2\right\} + 3\left\{\beta\bar{c}r + \beta J^{(1)}_{\varepsilon'}(r)r\right\}\right] \\
&\quad \times \left\{1 + O\left(\frac{1}{N'}\right)\right\} \\
&= \sum_r \exp\left[N'\bar{f}(r) + 3\left\{\beta\bar{c}r + \beta J^{(1)}_{\varepsilon'}(r)r\right\}\right]\left\{1 + O\left(\frac{1}{N'}\right)\right\}, \qquad (6.9)
\end{aligned}
$$

where

$$
J^{(1)}_{\varepsilon'}(r) = \left(\frac{1}{N'r}\sum_{k=1}^{N'r}\varepsilon'_k\right) \qquad (6.10)
$$

By the saddle point approximation, $A_\pm$ and A_{3+} are approximated as

$$
\begin{aligned}
A_\pm &\approx A\exp\left[\pm\left(\beta c\bar{r}_0 + \beta J^{(1)}_{\varepsilon'}(\bar{r}_0)\bar{r}_0\right)\right]\left\{1 + O\left(\frac{1}{N'}\right)\right\} \\
A_{3+} &\approx A\exp\left[3\left(\beta c\bar{r}_0 + \beta J^{(1)}_{\varepsilon'}(\bar{r}_0)\bar{r}_0\right)\right]\left\{1 + O\left(\frac{1}{N'}\right)\right\}.
\end{aligned} \qquad (6.11)
$$

By letting $N' = N$ for large N, we obtain,

$$
\begin{aligned}
\theta_1^{(2,AN)} &= 2\beta\left(h_1 - m\right) + 2\beta c\bar{r}_0 + 2\beta J^{(1)}_{\varepsilon'}(\bar{r}_0)\bar{r}_0 + O\left(\frac{1}{N}\right) \\
\theta_2^{(2,AN)} &= 2\beta\left(h_2 - m\right) + 2\beta c\bar{r}_0 + 2\beta J^{(1)}_{\varepsilon'}(\bar{r}_0)\bar{r}_0 + O\left(\frac{1}{N}\right) \\
\theta_{12}^{(2,AN)} &= \beta\left(J_{12} + J_{21}\right) + O\left(\frac{1}{N}\right).
\end{aligned} \qquad (6.12)
$$

By assuming that ε'_k is a random variable with the mean 0 and variance σ'^2,

$$
\varepsilon'_k \sim N\left(0, \sigma'^2\right), \qquad (6.13)
$$

the distribution of $J^{(1)}_{\varepsilon'}(\bar{r}_0)$ is estimated as

$$J^{(1)}_{\varepsilon'}(\bar{r}_0) = \frac{1}{N\bar{r}_0}\sum_{k=1}^{N\bar{r}_0}\varepsilon'_k \sim N\left(0, \frac{\sigma'^2}{N\bar{r}_0}\right). \tag{6.14}$$

Therefore, we obtain

$$\begin{aligned}
\theta_1^{(2,AN)} &= 2\beta\,(h_1 - m) + 2\beta c\bar{r}_0 + O\left(\frac{1}{N}\right)\\
\theta_2^{(2,AN)} &= 2\beta\,(h_2 - m) + 2\beta c\bar{r}_0 + O\left(\frac{1}{N}\right)\\
\theta_{12}^{(2,AN)} &= \beta\,(J_{12} + J_{21}) + O\left(\frac{1}{N}\right).
\end{aligned} \tag{6.15}$$

Finally, by assuming that ε_j is a random variable with the mean 0 and variance σ^2,

$$\varepsilon_j \sim N\left(0, \sigma^2\right), \tag{6.16}$$

the distribution of $h_\varepsilon(r)$ and $J_{\varepsilon'}(r)$ in equation 6.4 is estimated as

$$\begin{aligned}
h_\varepsilon(r) &\sim N\left(0, \frac{\sigma^2}{Nr}\right),\\
J_{\varepsilon'}(r) &\sim N\left(0, \frac{\sigma'^2}{(Nr)^2}\right).
\end{aligned} \tag{6.17}$$

Therefore, for the large N limit, equation 6.8 reduces to

$$\log\frac{1-\bar{r}_0}{\bar{r}_0} + 2\beta\left(\bar{h} - m\right) + 2\beta\overline{cr}_0 = 0, \tag{6.18}$$

which is the same as equation 5.6. Thus, by letting $\bar{r}_0 = r_0$, we obtain

$$\begin{aligned}
\theta_1^{(2,AN)} &= 2\beta\,(h_1 - m) + 2\beta c r_0 + O\left(\frac{1}{N}\right),\\
\theta_2^{(2,AN)} &= 2\beta\,(h_2 - m) + 2\beta c r_0 + O\left(\frac{1}{N}\right),\\
\theta_{12}^{(2,AN)} &= \beta\,(J_{12} + J_{21}) + O\left(\frac{1}{N}\right),
\end{aligned} \tag{6.19}$$

which is equivalent to equation 5.10. Finally, by defining the corrected first-order information-geometric measures as

$$\begin{aligned}\tilde{\theta}_1^{(2,AN)} &= \theta_1^{(2,AN)} - 2\beta c r_0,\\ \tilde{\theta}_2^{(2,AN)} &= \theta_2^{(2,AN)} - 2\beta c r_0,\end{aligned} \tag{6.20}$$

they provide consistent approximation of the external inputs,

$$\begin{aligned}\tilde{\theta}_1^{(2,AN)} &= 2\beta\,(h_1 - m) + O\left(\frac{1}{N}\right),\\ \tilde{\theta}_2^{(2,AN)} &= 2\beta\,(h_2 - m) + O\left(\frac{1}{N}\right).\end{aligned} \tag{6.21}$$

In summary, the corrected first-order information-geometric measures ($\tilde{\theta}_1^{(2,AN)}$ and $\tilde{\theta}_2^{(2,AN)}$) and the second-order information geometric-measure $\theta_{12}^{(2,AN)}$ provide consistent approximation of the external inputs and the connection strengths, respectively. In other words, the corrected first- and second-order information-geometric measures of the two-neuron log-linear model are proven to provide useful insights into the network architectures even in the case of nonuniformly connected asymmetric networks.

7 Discussion

We have investigated the relationship between the information-geometric measures and two network parameters, corresponding to the connection strengths and the external inputs, in an N neuron network. We focused on the information-geometric measures given by the two-neuron log-linear model because it is the simplest of all possible information-geometric measures and can be estimated rather easily in real experimental settings. Using a stochastic binary model neural network in the equilibrium state, we derived an explicit relationship between the measures $\theta^{(2)}$ and the network parameters for symmetrically connected networks (see equation 4.9) and simplified it for uniformly connected networks (see equation 5.1). Then in the large N limit, we estimated the accuracy of the information-geometric measures. We showed that the information-geometric measures provided a consistent approximation of the network parameters for both uniformly connected (see equations 5.17 and 5.19) and nonuniformly and asymmetrically connected networks (see equations 6.19 and 6.21). These results therefore suggest that the corrected first- and second-order information-geometric measures of the two-neuron log-linear model provide useful insights into the underlying network architecture.

In this letter, we considered only the lag-zero information-geometric measure, $\theta_{12}^{(2)} = \theta_{12}^{(2)}(0)$, as an estimator of the connection strength. We could extend the measure to the time-lagged information-geometric measure $\theta_{12}^{(2)}(\tau)$. As previous studies (Ginzburg & Sompolinsky, 1994; Tatsuno & Okada, 2004) suggest, the time-lagged measure would provide information about the directionality of connections. Therefore, one of the future directions to take will be to investigate the time-lagged information-geometric measure $\theta_{12}^{(2)}(\tau)$ and estimate the directionality of asymmetrically connected networks. In addition, in this study, we considered only the case of random gaussian connections with small variance. It is therefore interesting to investigate the case with large variance, for example, the regime in which the system becomes glassy, in the future.

Regarding the number of neurons included in the log-linear model, we focused on the two-neuron log-linear model. When an experimental situation allows only a limited number of trials, the two-neuron log-linear model will provide a robust estimation of all three parameters: $\theta_1^{(2)}$, $\theta_2^{(2)}$, and $\theta_{12}^{(2)}$. As the previous study indicated (Tatsuno & Okada, 2004), however, if a larger number of trials is available, the higher-order log-linear model is expected to provide better estimations. Thus, it is interesting to extend the result of this study to a higher-order log-linear model in the future.

Our previous work showed that the information-geometric measures could not disentangle the connection strengths and the external inputs correctly for asymmetrically connected networks (Tatsuno & Okada, 2004). On the other hand, our previous biophysical simulations indicated that they indeed estimated the relative change of connection strengths and external inputs successfully even with asymmetric connections (Lipa et al., 2006, 2007). This study explains this apparent discrepancy. The discrepancy between these two works arises because the former study used a network of only a couple of neurons in a high-firing-rate range where the estimation error is high. The latter study used a network of 10 neurons in a low but realistic firing-rate range where the error is smaller. Both studies used the uncorrected information-geometric measures. In this letter, we showed that the corrected information-geometric measures can indeed approximate the network parameters regardless of firing-rate range.

The second-order information-geometric measure of the two-neuron log-linear model $\theta_{12}^{(2)}$ can be considered an alternative to the correlation coefficient to quantify the statistical dependence between two binary random variables. Both $\theta_{12}^{(2)}$ and the correlation coefficient are calculated from two spike trains, but $\theta_{12}^{(2)}$ has significant advantages; it can quantify pure interactions that are independent of the mean firing-rate modulations, and it provides a consistent approximation of the connection strengths, as we showed in this letter. These two properties of the information-geometric measures will be very useful when applied to multineuronal electrophysiological

data. With the information-geometric measures, neuronal assemblies that exhibit increased pure correlations can be detected and may lead to the identification of neuronal subgroups that play important cognitive functions. Furthermore, assessment of the connection strengths by the information-geometric measures may lead, for the first time, to estimates on network changes from in vivo recordings and thus is expected to have a significant impact on the study of learning and memory consolidation (Lipa et al., 2006, 2007).

In this letter, we chose the value of model parameters β and m. In practice, these parameters should be calculated from spike train data. Generally, however, this task may be an ill-posed problem because multiple sets of parameters may produce the same spike trains. But because p_{00}, p_{01},p_{10}, p_{11}, and mean firing rate S_i can be estimated from the data, they may be used for the model parameter estimation. For example, for a uniform connection case, the following equations are obtained:

$$p_{00} = \frac{\exp\left[-\beta c S\right]}{\exp\left[-\beta c S\right] + \exp\left[2\beta\left(h-m\right) + c S\right] + \exp\left[2\frac{c}{N} + 3c S + 4\beta\left(h-m\right)\right]},$$

$$p_{01} = p_{10} = \frac{\exp[2\beta(h-m) + c S]}{\exp[-\beta c S] + \exp[2\beta(h-m) + c S] + \exp[2\frac{c}{N} + 3c S + 4\beta(h-m)]},$$

$$p_{11} = \frac{\exp\left[2\frac{c}{N} + 3c S + 4\beta\left(h-m\right)\right]}{\exp\left[-\beta c S\right] + \exp\left[2\beta\left(h-m\right) + c S\right] + \exp\left[2\frac{c}{N} + 3c S + 4\beta\left(h-m\right)\right]},$$

$$\log\frac{1-S}{S} + 2\beta\left(h-m\right) + 2\beta c S = 0. \tag{7.1}$$

Assuming that N is a typical number of synaptic inputs in the neocortex (i.e., between 5,000 and 10,000), these equations can be solved for β, m, c, and h. Obtaining analytical solutions may be difficult because this is a set of four nonlinear equations, but they can be solved numerically. Although the calculations for general asymmetric connections are more difficult, our biophysical simulation using the NEURON simulator suggests that relative changes of connection strengths and external inputs can be estimated from spike train data (Lipa et al., 2006, 2007). Electrophysiological experiments could therefore use such an analysis to determine whether connection strengths are modified by experience. In summary, with values of β and r_0 estimated from spike trains, the bias correction term of the information-geometric measures can also be estimated. This makes the method valuable not only theoretically but also in practice.

To understand how the brain works in terms of groups of interacting neurons, further development of analytical techniques and recording technology is necessary. The information-geometric method is a promising analytical technique and will provide a useful tool for spike train analysis in both in vitro and in vivo recordings.

Acknowledgments

We thank Bruce L. McNaughton, Peter Lipa, Masato Okada, and Toshiaki Omori for useful discussion and critical reading of the manuscript and two anonymous reviewers for helpful comments and suggestions. This work was supported by the National Institutes of Health (MH46823).

References

Abeles, M., & Gerstein, G. L. (1988). Detecting spatiotemporal firing patterns among simultaneously recorded single neurons. *J. Neurophysiol.*, *60*(3), 909–924.

Aertsen, A. M., Gerstein, G. L., Habib, M. K., & Palm, G. (1989). Dynamics of neuronal firing correlation: Modulation of "effective connectivity." *J. Neurophysiol.*, *61*(5), 900–917.

Amari, S. (1985). *Differential geometrical methods in statistics*. Berlin: Springer-Verlag.

Amari, S. (2001). Information geometry on hierarchy of probability distributions. *IEEE Transactions on Information Theory*, *47*(5), 1701–1711.

Amari, S., & Nagaoka, H. (2000). *Methods of information geometry*. New York: Oxford University Press.

Amari, S., Nakahara, H., Wu, S., & Sakai, Y. (2003). Synchronous firing and higher-order interactions in neuron pool. *Neural Comput.*, *15*(1), 127–142.

Brown, E. N., Kass, R. E., & Mitra, P. P. (2004). Multiple neural spike train data analysis: State-of-the-art and future challenges. *Nat. Neurosci.*, *7*(5), 456–461.

Buzsaki, G. (2004). Large-scale recording of neuronal ensembles. *Nat. Neurosci.*, *7*(5), 446–451.

Czanner, G., Grün, S., & Iyengar, S. (2005). Theory of the snowflake plot and its relations to higher-order analysis methods. *Neural Comput.*, *17*(7), 1456–1479.

Eleuteri, A., Tagliaferri, R., & Milano, L. (2005). A novel information geometric approach to variable selection in MLP networks. *Neural Netw.*, *18*(10), 1309–1318.

Fellous, J. M., Tiesinga, P. H., Thomas, P. J., & Sejnowski, T. J. (2004). Discovering spike patterns in neuronal responses. *J. Neurosci.*, *24*(12), 2989–3001.

Gerstein, G. L., & Perkel, D. H. (1969). Simultaneously recorded trains of action potentials: Analysis and functional interpretation. *Science*, *164*(881), 828–830.

Ginzburg, I. I., & Sompolinsky, H. (1994). Theory of correlations in stochastic neural networks. *Physical Review, E, Statistical Physics, Plasmas, Fluids, and Related Interdisciplinary Topics*, *50*(4), 3171–3191.

Grün, S., Diesmann, M., & Aertsen, A. (2002). Unitary events in multiple single-neuron spiking activity: I. Detection and significance. *Neural Comput.*, *14*(1), 43–80.

Hoffman, K. L., & McNaughton, B. L. (2002). Coordinated reactivation of distributed memory traces in primate neocortex. *Science*, *297*(5589), 2070–2073.

Houghton, C., & Sen, K. (2008). A new multineuron spike train metric. *Neural Comput.*, *20*, 1495–1511.

Ikeda, K. (2005). Information geometry of interspike intervals in spiking neurons. *Neural Comput.*, *17*(12), 2719–2735.

Kass, R. E., Ventura, V., & Brown, E. N. (2005). Statistical issues in the analysis of neuronal data. *J. Neurophysiol.*, *94*(1), 8–25.

Lipa, P., Tatsuno, M., Amari, S., McNaughton, B. L., & Fellous, J. M. (2006). A novel analysis framework for characterizing ensemble spike patterns using spike train clustering and information geometry. *Soc. Neurosci. Abstr.*, *36:371*, 6.

Lipa, P., Tatsuno, M., McNaughton, B. L., & Fellous, J. M. (2007). Dynamics of neural assemblies involved in memory-trace replay. *Soc. Neurosci. Abstr.*, *37.308*, 13.

Louie, K., & Wilson, M. A. (2001). Temporally structured replay of awake hippocampal ensemble activity during rapid eye movement sleep. *Neuron*, *29*(1), 145–156.

Miura, K., Okada, M., & Amari, S. (2006). Estimating spiking irregularities under changing environments. *Neural Comput.*, *18*(10), 2359–2386.

Nadasdy, Z., Hirase, H., Czurko, A., Csicsvari, J., & Buzsaki, G. (1999). Replay and time compression of recurring spike sequences in the hippocampus. *J. Neurosci.*, *19*(21), 9497–9507.

Nakahara, H., & Amari, S. (2002). Information-geometric measure for neural spikes. *Neural Comput.*, *14*(10), 2269–2316.

Nakahara, H., Amari, S., & Richmond, B. J. (2006). A comparison of descriptive models of a single spike train by information-geometric measure. *Neural Comput.*, *18*(3), 545–568.

Nicolelis, M. A., & Ribeiro, S. (2002). Multielectrode recordings: The next steps. *Curr. Opin. Neurobiol.*, *12*(5), 602–606.

Riehle, A., Grün, S., Diesmann, M., & Aertsen, A. (1997). Spike synchronization and rate modulation differentially involved in motor cortical function. *Science*, *278*(5345), 1950–1953.

Shimazaki, H., & Shinomoto, S. (2007). A method for selecting the bin size of a time histogram. *Neural Comput.*, *19*(6), 1503–1527.

Tatsuno, M., Lipa, P., & McNaughton, B. L. (2006). Methodological considerations on the use of template matching to study long-lasting memory trace replay. *J. Neurosci.*, *26*(42), 10727–10742.

Tatsuno, M., & Okada, M. (2004). Investigation of possible neural architectures underlying information-geometric measures. *Neural Comput.*, *16*(4), 737–765.

Wilson, M. A., & McNaughton, B. L. (1993). Dynamics of the hippocampal ensemble code for space. *Science*, *261*(5124), 1055–1058.

Zhang, K., Ginzburg, I., McNaughton, B. L., & Sejnowski, T. J. (1998). Interpreting neuronal population activity by reconstruction: Unified framework with application to hippocampal place cells. *J. Neurophysiol.*, *79*(2), 1017–1044.

Received April 4, 2008; accepted January 8, 2009.